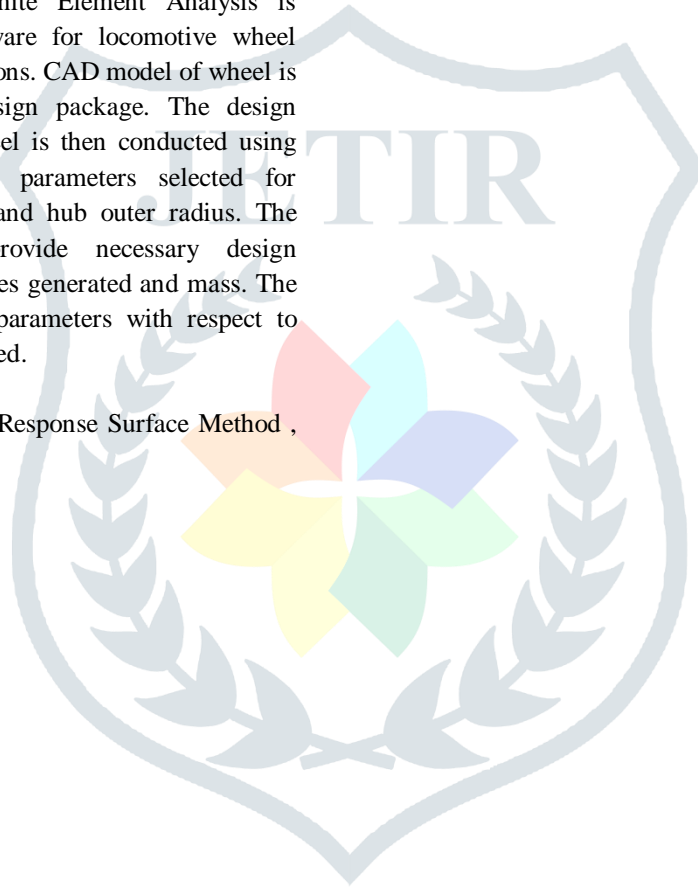


Design Optimization of locomotive wheel by varying Hub inner radius and hub outer radius

¹Harmesh Lal, ²Dr. Balkar Singh
^{1,2}Department of Mechanical Engineering
^{1,2}IKPTU Jalandhar

Abstract– The service life of locomotive wheels, rail is largely dependent upon cracks initiation and propagation. The determining factors for these two parameters are contact stresses between locomotive wheel and track. The research investigates the stresses generated in locomotive wheel under dynamic conditions. Finite Element Analysis is conducted using ANSYS software for locomotive wheel under transient structural conditions. CAD model of wheel is developed using Creo 2.0 design package. The design optimization of locomotive wheel is then conducted using response surface method and parameters selected for analysis are hub inner radius and hub outer radius. The findings of the research provide necessary design modifications to minimize stresses generated and mass. The sensitivity of both the design parameters with respect to output parameters is also evaluated.

Keywords: Locomotive wheel, Response Surface Method , FEA, ANSYS, Contact Stresses



I. INTRODUCTION

Contact is the principal method of applying loads between deformable solids, and therefore is present in a wide variety of mechanical components. In addition, contacts usually act as stress concentrations, and are thus probable locations for mechanical failure. Contact stresses developed during the pressing action of two bodies needs careful attention since occurrences of such forces are very frequent. Considering the gears, ball & roller bearings, when two bodies with curved surfaces come into contact without any pressure or forces between them, the geometry of contact is in general either a point or a line. These contact stresses are unavoidable phenomenon in railway systems. It is difficult to measure the contacting pressure due to curve on track, load applied. Wheel-rail contact is always a hot topic for railway vehicle dynamics researchers and wheel-track maintenance engineers. The determination of forces acting between wheel and rail is definitely the most important question for the study of dynamic behavior of a railway vehicle. The contact area shape for loco wheel case is elliptical in shape. The contact area between rail wheel system is of elliptical shape. The contact elliptical area is small so stresses developed will be higher. The stress evaluation for wheel rail contact is done using hertz theory which states that when two solid materials are compressed to each other by vertical loads, their contact area is formed. Shape and the value of the contact area between two elastic materials are at static mode.



Fig 1:Locomotive wheel

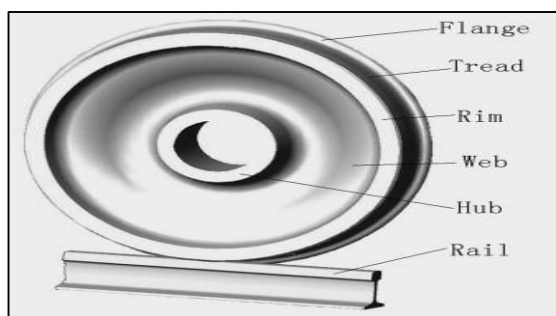


Fig2:Locomotive wheel [1]

Figure 2 above shows naming of various parts of

wheel rail system. As its evident the immediate contact pair is between tread, flange and rail track.

II. RESEARCH OBJECTIVES

The objective of this research is to determine the frictional stresses due to wheel rail contact and optimize design of locomotive wheel using response surface method to minimize contact stress under dynamic conditions.

III. METHODOLOGY

The transient structural analysis is conducted using ANSYS 18.1 software which is based on Finite Element Analysis. Finite Element Analysis constitutes 3 stages which are preprocessing, solution and postprocessing. The dimensions of locomotive wheel is taken from KLV data sheet as shown in figure 3 below.

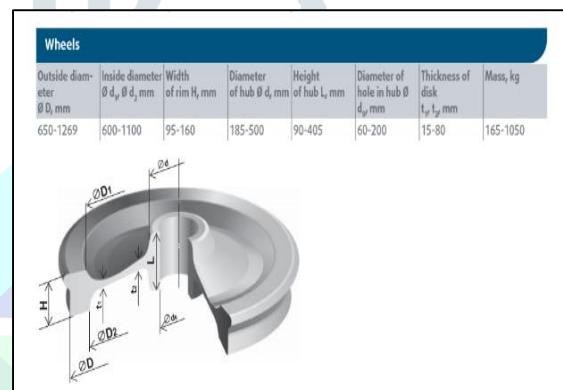


Fig3:Wheel dimension range [4]

Table 1 below shows material properties of wheel and axle load. The axle load specified in table 1 below is used for structural and fatigue life analysis.

Table 1: Material properties and Loads

| | |
|-------------------|------------------------|
| Axle Load | 146.2 KN |
| Young's Modulus | 205GPa |
| Density | 7850 Kg/m ³ |
| Ultimate Strength | 450MPa |
| Yield Strength | 250MPa |

The CAD model of locomotive wheel and track is modeled using data reference ranges provided in figure 3. The full CAD model developed of locomotive wheel is developed using Creo 2.0 software. The Creo 2.0 is design package developed by PTC (Parametric Technology Corporation) and has properties of parent child relationship along with bidirectional associativity.

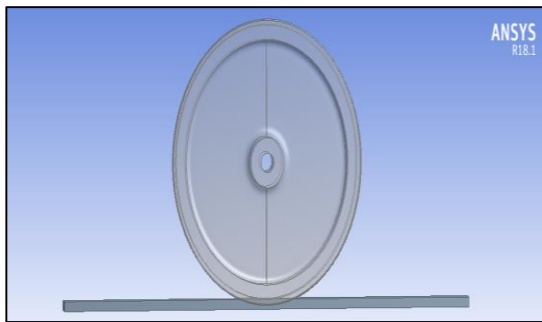


Fig4:CAD model of wheel and track

The domain meshing is performed using tets elements as shown in in fig 5 below. Element count is158468 and node count is251682. Inflation settings, smoothing settings and transition ratio are all set to medium.

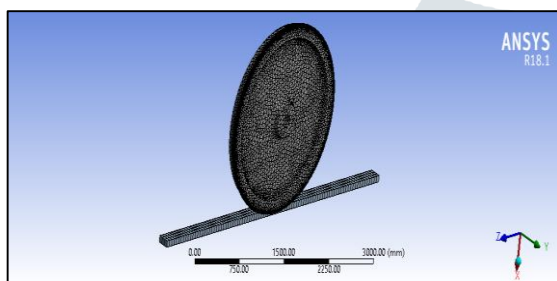


Fig5:Meshed model of wheel and track

The tetrahedral element shape is shown in figure 6 below. The element shown below consists of 4 nodes as shown in figure 6 below.

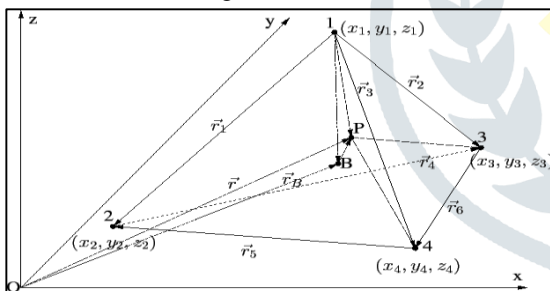


Fig 6:Element shape of Tetrahedral Element

The shape of tetrahedral element as shown in figure 6 consists of 4 nodes having 3 degrees of freedom per node. These are U_x , U_y and U_z which are formulated in 3D space. The frictional contact pair is defined between wheel and rail as shown in figure 7 below.

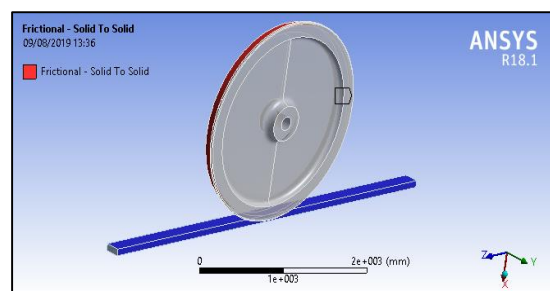


Fig 7:Frictional contact between wheel and rail

For defining frictional contact pair the locomotive wheel surface is selected as contact body and track as target body as shown in figure 8 below.

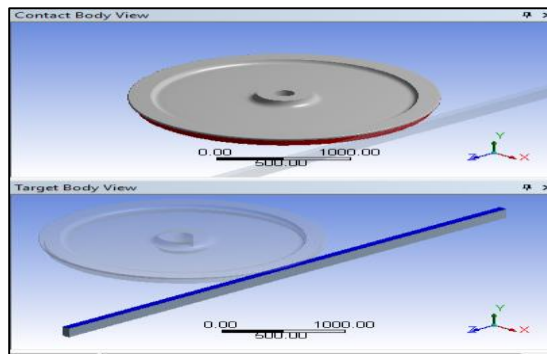


Fig 8:Contact body and target body

| Scope | |
|---|------------------|
| Scoping Method | Geometry Sele... |
| Contact | 3 Faces |
| Target | 2 Faces |
| Contact Bodies | Solid |
| Target Bodies | Solid |
| Definition | |
| Type | Frictional |
| <input type="checkbox"/> Friction Coefficient | 0.25 |
| Scope Mode | Automatic |

Fig 9:Frictional type contact

The contact pair defined between wheel and rail is frictional type as shown in figure 9 above. The coefficient of friction(μ) defined is .25 as shown in figure 9 above. Fixed support is applied on bottom surface of track, frictionless support is applied on side face of wheel while downward force of 146200N is applied on inner hub surface. The loading conditions are shown in figure 10 below.

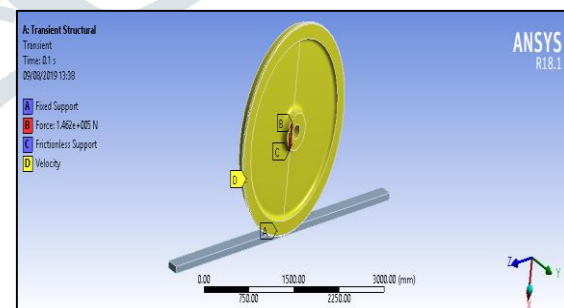


Fig 10:Loads and Boundary Conditions

The contact pair analysis involves non linearity which required newton Raphson algorithm to solve.

The single equation variable can be written as

$$f(x) = 0 \quad (1)$$

The iteration formula of Newton-Raphson is given by

$$x^{(j+1)} = x^j - \frac{f(x^j)}{f'(x^j)} \quad (2)$$

where,

$$f'(x^j) = \frac{df}{dx}(x^j) \quad (3)$$

Starting with an initial guess x^0 we compute x^1 from the equation (2). We use this equation successively until x^j converges to the solution x^* .

Equation (2) can be written in the form shown below

$$f(x^j) + f'(x^j)(x^{j+1} - x^j) = 0 \quad (4)$$

and consider the function

$$y = f(x^j) + f'(x^j)(x - x^j) \quad (5)$$

The above equation (5) represents a straight line passing through the point $(x^j, f(x^j))$ with the slope $f'(x^j)$. Thus, the straight line is the tangent to the curve $y = f(x)$.

For $x = x^{(j+1)}$ it holds $y = 0$.

Hence, x^{j+1} is a point of intersection of the tangent with the Ox axis. The geometric interpretation of Newton-Raphson method is shown in Fig. 11

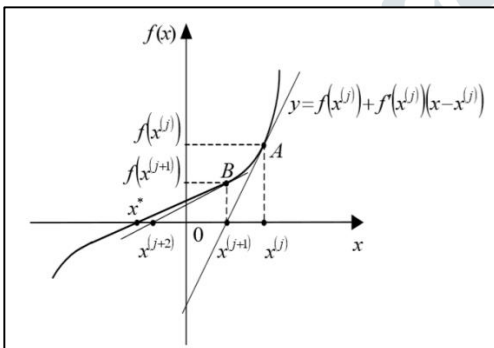


Figure 11: Geometric interpretation of Newton-Raphson method

The Newton-Raphson computation process is continued until $x^{j+1} - x^j \cong 0$

$$x^{j+1} - x^j = \frac{f(x^j)}{f'(x^j)}$$

Then the equation

$$x^{j+1} - x^j = 0$$

Implies

$$f(x^j) = 0$$

Thus, we assume

$$x^j \cong x^*$$

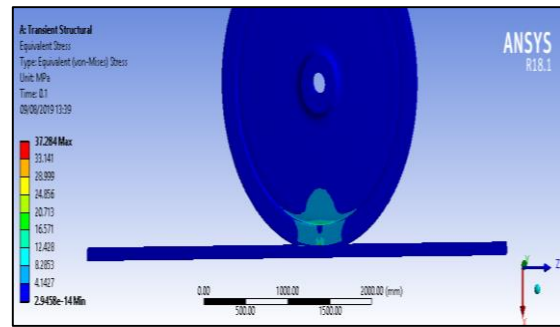


Fig 12:Equivalent stress plot

The equivalent stress plot is shown in figure 12 above shows maximum stress value of 37.28MPa at the point of contact in elliptical shape.

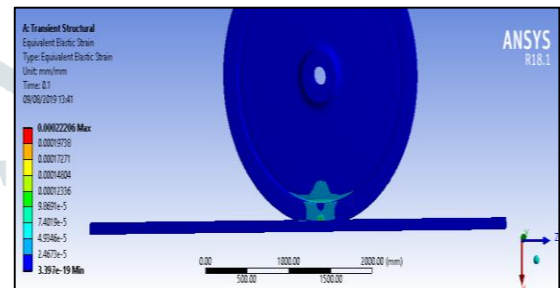


Fig 13:Equivalent elastic strain

The maximum equivalent elastic strain generated is .00022 and in contact zone between wheel and rail.

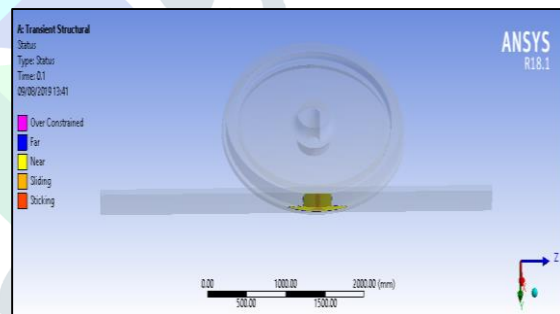


Fig 14:Equivalent elastic strain

The contact status as shown in figure 14 above shows near status (light yellow) near contact zone and sliding at the zone of contact shown by dark yellow color.

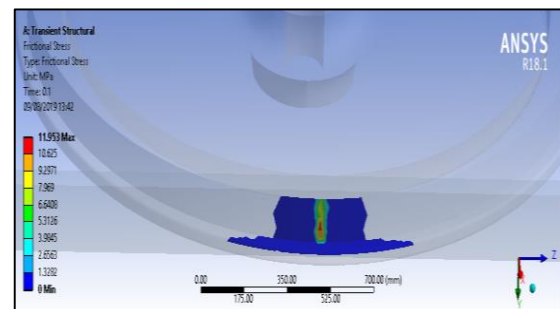


Fig 15:Frictional stress

The frictional stress plot shown in figure 15 above shows maximum stress value of 11.953Mpa at the

point of contact and reduces to 9.297Mpa away from point of contact which further reduces on moving away from point of contact.

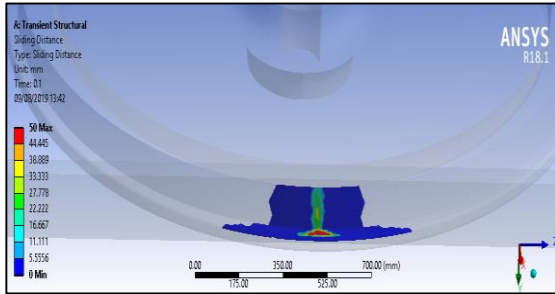


Fig 16:Sliding distance

The sliding distance obtained from analysis is shown in figure 16 above shows maximum magnitude of 50mm on lateral member of wheel.

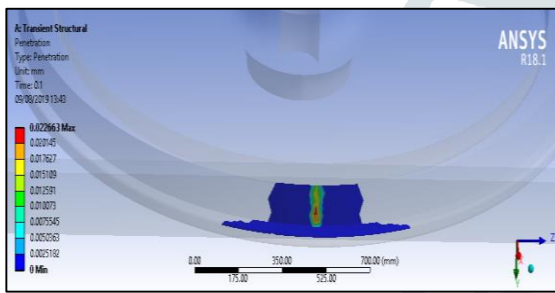


Fig 17:Penetration

The maximum penetration obtained from analysis as shown in figure 16 above shown maximum magnitude of .022mm at the point of contact and reduces on moving away from contact zone. The penetration value reduces to .015 on tread inner face.

IV. OPTIMIZATION USING RESPONSE SURFACE METHODOLOGY

In Response Surface Methodology, mathematical and statistical techniques are employed for empirical model building [5]. The responses which are output variable are optimized on the basis of input variable which are independent. The independent variables are denoted by $x_1, x_2, x_3, \dots, x_n$. These variables are independent and controlled by experimenter with negligible error. The relationship between independent variable and dependent variable can be expressed as

$$y = f(x_1, x_2, x_3, \dots, x_n) + \epsilon$$

Where ϵ is error observed in the response y

The response of design which is function of multiple design variables (x_i), the response surface behavior can be expressed by the approximation as a polynomial $y = f(x)$ on the basis of observation data. The two variable regression model

of quadratic response is given by

$$y = \beta_0 + \beta_1 x_1 + \beta_2 x_2 + \beta_3 x_1^2 + \beta_4 x_2^2 + \beta_5 x_1 x_2$$

where $\beta_0, \beta_1, \beta_2, \beta_3, \beta_4$ and β_5 are the regression coefficients. The response surface optimization of the current research deals with 2 design parameters which are hub inner radius (x_1) and hub outer radius (x_2). To establish the cause and effect relationship design of experiments (DOE) is performed using ANSYS software. These experiments are conducted using central composite design method or CCD.

| | A | B | C | D | E | F | G | H |
|----|------|----------------|----------------|-------------------------------------|---------------------------------|-------------------------------------|---------------------------------------|--------------------|
| 1 | Name | P20-Outer (mm) | P20-Inner (mm) | P20-Equivalent Stress Maximum (MPa) | P20-Radial Stress Maximum (MPa) | P20-Tangential Stress Maximum (MPa) | P20-Equivalent Stress 2 Maximum (MPa) | P20-Side Mass (kg) |
| 2 | 1 | 100 | 125 | 37.265 | 11.933 | 0.02263 | 27.018 | 296 |
| 3 | 2 | 72 | 125 | 44.33 | 15.122 | 0.02078 | 25.363 | 235.8 |
| 4 | 3 | 88 | 125 | 41.837 | 15.727 | 0.02087 | 26.491 | 232.1 |
| 5 | 4 | 88 | 112.5 | 45.123 | 15.084 | 0.02082 | 25.447 | 241.3 |
| 6 | 5 | 88 | 137.5 | 45.812 | 15.018 | 0.02096 | 25.343 | 247 |
| 7 | 6 | 72 | 112.5 | 46.434 | 14.689 | 0.0208 | 25.495 | 246.7 |
| 8 | 7 | 88 | 112.5 | 45.326 | 15.085 | 0.02082 | 25.521 | 232.6 |
| 9 | 8 | 72 | 137.5 | 45.124 | 15.022 | 0.02099 | 25.32 | 236.5 |
| 10 | 9 | 88 | 137.5 | 44.318 | 15.141 | 0.02146 | 25.34 | 233.5 |

Fig 18:Hub inner radius and hub outer radius optimization

By using the least square methodology after design of experiments (DOE) the response surface is generated. This response surface is generated using all input and output variables. Optimization is performed using the data points fitted with 2nd order polynomial. Figure below shows the goodness of fit plots for all the subsystems.

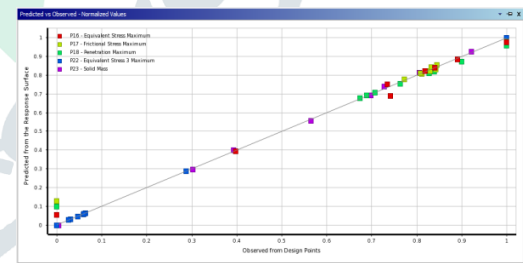


Fig 19:Goodness of fit curve

The goodness of fit curve of linear regression model shows the difference between the observed values and expected values of output quantities. It also describes the accuracy of prediction for future set of observations. The plot type is of X-Y scatter showing the difference between data points and linear fit.

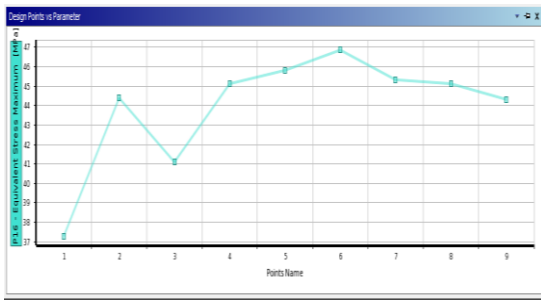


Fig 20:Equivalent stress at different design points

The above graph shows equivalent stress at different design points (x_1 : hub inner radius and x_2 : hub outer radius). The equivalent stress is found to be maximum at design point number 6 in which hub inner radius is 72mm and hub outer radius is 112.5mm.

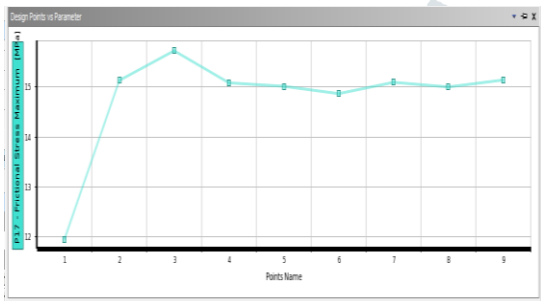


Fig 21:Frictional stress at different design points

The maximum frictional stress obtained is noticed for design point 3 (hub inner radius 88mm and hub outer radius 125mm) while minimum frictional stress is noticed for design point 1 (hub inner radius 72mm and hub outer radius 125mm)

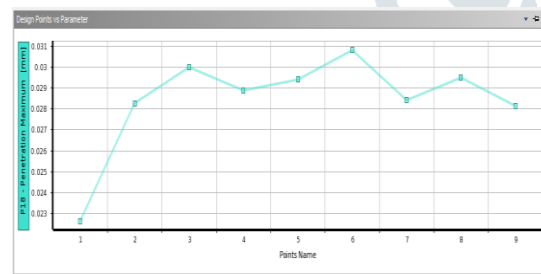


Fig 22:Penetration at different design points

From the penetration curve obtained at different design points shows that maximum penetration is observed for design point number 6 having hub inner radius 72mm and hub outer radius 112.5mm. The magnitude of penetration is .0308mm and minimum penetration is for design point 1 with magnitude of .0226mm.

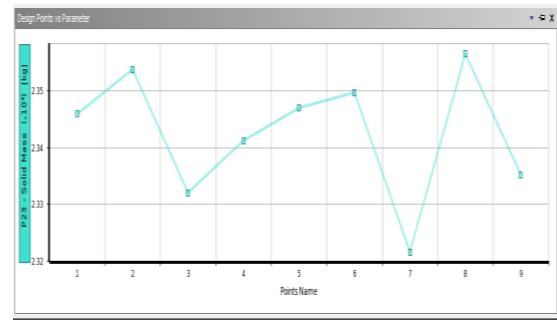


Fig 23:Solid mass at different design points

From the solid mass curve obtained at different design points shows that maximum mass is observed for design point number 8 having hub inner radius 72mm and hub outer radius 137.5mm. The minimum mass is obtained for point 7 having hub inner radius 88mm and hub outer radius 112.5mm.

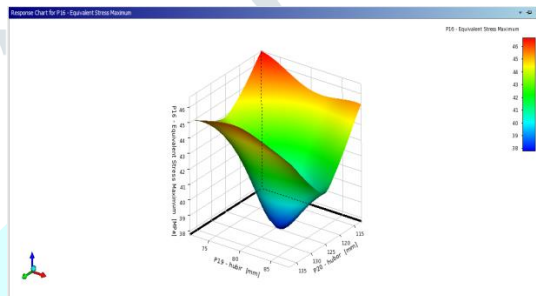


Fig 24:Response surface chart for equivalent stress

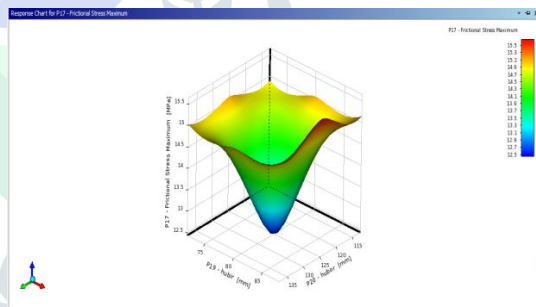


Fig 25:Response surfacegraph for frictional stress

The response surface charts are plotted for equivalent stress and frictional stress as shown in figure 16 and figure 17 above. The equivalent stress plot shows that maximum stress is obtained for hub inner radius less than 75mm. The hub outer radius range from 115mm to 120mm shows maximum equivalent stress. The maximum frictional stress is noticed for hub inner radius range of 80mm to 85mm and hub outer radius range from 120mm to 135mm.

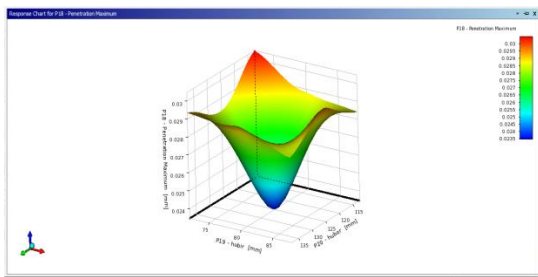


Fig 26: Response surface graph for penetration

The response surface plot for penetration is shown in figure 26 above. The maximum magnitude of penetration is noticed for hub inner radius less than 75mm and hub outer radius less than 120mm.

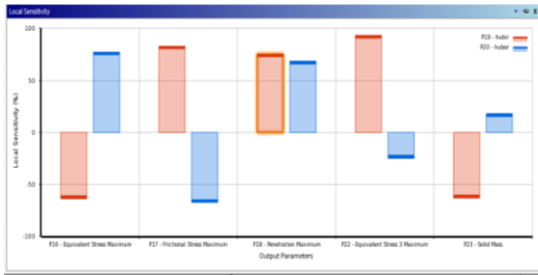


Fig 27: Sensitivity plot for different variables

The sensitivity of different variables is shown in figure 27 above. For equivalent stress hub inner radius shows 63.72%(negative) sensitivity and hub outer radius shows 77.38%(positive) sensitivity. For frictional stress hub inner radius shows 83.14%(positive) sensitivity and hub outer radius shows 67.25%(negative) sensitivity. For equivalent stress hub inner radius shows 93.55%(positive) sensitivity and hub outer radius shows 24.87%(negative) sensitivity. For solid mass hub inner radius shows 63.03%(negative) sensitivity and hub outer radius shows 18.26%(positive) sensitivity.

V CONCLUSION

The transient structural analysis is performed using ANSYS software to determine frictional stress, equivalent stress. The response surface optimization predicted the design points for stress (equivalent and frictional) and mass minimization. The sensitivity plots generated gives crucial information on sensitivity of different optimization parameters i.e hub inner radius and hub outer radius. The minimum mass obtained from analysis is 2321.6Kg.

REFERENCES:

- [1] M.R. Zhang, H.C. Gu, 2008, Fracture Toughness of nanostructured railway wheels; Engineering Fracture Mechanics, 5113–5121
- [2] “ANSYS” <http://www.ansys.com>
- [3] Pramod Murali Mohan, 2012, Analysis of Railway

Wheel to study Thermal and Structural Behavior, Published in International Journal of Scientific & Engineering Research, Volume 3, Issue 11

[4]KJLW

[5] Box, E.P., and Draper, N.R. (1987) Empirical Model-building and Response Surfaces, John Wiley.-k

